Changes in Signal Morphology of Hand-held ECG Devices with Dry Electrodes

Markus Lueken[1], Matthias D Zink[2], Steffen Leonhardt[1]

[1] Medical Information Technology (MedIT), Helmholtz-Institute for Biomedical Engineering, RWTH Aachen University, Aachen, Germany
[2] Department of Internal Medicine I-Cardiology, University Hospital RWTH, Aachen, Germany, Cardiology and Angiology, Medical Center, Faculty of Medicine, University of Freiburg, Freiburg, Germany, and the Department of Cardiology, Pneumology, Angiology, Acute Geriatrics, Intensive Care and Thoracic Surgery, Ortenau Klinikum Lahr/Offenburg, Lahr/Schwarzwald, Germany

Abstract

Hand-held ECG devices often comprise dry electrodes for establishing an electrical connection to the patient's body. Due to motion artifacts, static electrode charges and DC amplifier offsets, these devices usually incorporate signal conditioning, such as filter stages, which can affect the ECG signal morphology. In this work, we implemented a MATLAB Simscape-based model to simulate the electrode-skin interface of dry electrodes and the corresponding measurement pathway of a hand-held ECG measurement device to investigate the influence of skin impedance, geometric factors and electrical circuitry on the signal morphology of an Einthoven I-lead heart cycle prototype. We performed synchronized measurements with the commercially available ECG device MyDiagnostick and a Philips patient monitor MX800 for reference purposes to identify device-related signal distortions. Results indicate a significant change in signal morphology of the ECG, exhibiting an increasingly biphasic P-wave with reduced amplitude, a negative S-peak and an inverted T-wave.

1. Introduction

Devices for measuring ECG on a large scale, like handheld or wearable single-lead devices, gain importance in diagnosing cardiac arrhythmia, such as atrial fibrillation (AF) [1]. They depend on simple, typically dry electrode implementations and signal acquisition to realize an easily applicable recording of the electrical heart activity. The electrode characteristics play a crucial role in ensuring accurate signal acquisition. They must exhibit low impedance and high signal-to-noise ratio (SNR) to effectively capture electrophysiological signals and provide a robust measurement and reliable signal quality. Dry electrodes and their respective signal conditioning circuits often implement a high-pass characteristic, which has a potentially significant influence on the ECG signal morphology and, thus, on the diagnostic capabilities and possible misdiagnosis by the clinical expert due to misleading signal morphology. Additionally, when applying pre-trained neural networks initially trained on conventional ECG data, these signal morphology changes must be considered.

As was already shown in a previous analysis by our group, the MyDiagnostick device (Applied Biomedical Systems, Maastricht, The Netherlands) has certain limitations that require careful examination of the raw ECG data [2]. A primary concern is the effect of the input high-pass filter on the measurement signal, which influences both amplitude and morphology, particularly impacting the P-wave, S-wave, and T-wave components. Noise artifacts of similar amplitudes can further obscure these waveforms, making P-waves particularly challenging to identify. This issue becomes more pronounced in ECG recordings of lower quality, leading to unreliable detection of AF when discernible P-waves are absent. In contrast, QRS complexes retain distinct characteristics that facilitate identification through established peak detection algorithms such as the Pan-Tompkins algorithm [3]. Although the MyDiagnostick device thus provides highly reliable detection of AF based on the R-R interval variability [4], the specific changes in signal morphology need to be further investigated before a more semantic signal interpretation can be carried out based on evidence-based guidelines.

2. Methods & Material

2.1. Measurement Device

In this work, a handheld device (MyDiagnostick, Applied Biomedical Systems, Maastricht, The Netherlands), shown in Fig. 1, typically used for large-scale ECG data collection was analyzed concerning its signal distortion properties. It collects 1-minute ECG data of the patient equivalent to the Einthoven I-lead. This device facilitates the diagnosis of AF through automated analysis and detection of irregular heart rhythms, allowing for unsupervised and user-friendly screening for AF. Users hold the device by its metal electrodes to capture the ECG signal at a sampling rate of $f_{\text{s,stick}} = 200\,\text{Hz}$. The internal software analyzes the ECG signal to detect AF-related abnormalities or arrhythmia. The MyDiagnostick has proven to be a reliable and effective tool for the diagnosis of cardiac arrhythmia and has shown high correlation with standard 12-lead ECG measurements in recent studies [1, 4, 5].

Figure 1. Measurement device used in this work consisting of two dry metal electrodes and an LED-based visual decision feedback to communicate the diagnosis.

2.2. Data Recording

We have recorded ECG data of a healthy young subject to investigate the effect of the underlying measurement device incorporating dry electrodes and the associated filtering stages. Reference data of the Einthoven I-lead was recorded using a Philips MX800 patient monitor with a sampling frequency of $f_{\text{s,ref}} = 250\,\text{Hz}$. For this purpose, the subject was equipped with standard Ag/AgCl ECG electrodes. Data was recorded synchronously, and the one-minute interval of the MyDiagnostick measurement was included in the reference recording. To provide an accurate synchronization of both recordings, the subject was asked to perform a deep breathing maneuver with eight breaths per minute to enforce higher variability in the R-R intervals due to the respiratory sinus arrhythmia (RSA). R-peak amplitude and segment timings are also modulated by the RSA and provide higher variability for a more comprehensive investigation. The recorded reference data was resampled to $f_{\text{s,stick}}$ and both recordings were filtered according to IEC 60601-2-27 using a Butterworth band-pass filter with cut-off frequencies at $f_{\text{BP,high}} = 0.67\,\text{Hz}$ and $f_{\text{BP,low}} = 40\,\text{Hz}$. Afterward, the recordings were synchronized by calculating the correlation coefficient for different lags and identifying the maximum correlation. An exemplary recording of synchronized data from a patient monitor and hand-held device over one breathing cycle is shown in Fig. 2.

2.3. Electrode Modeling

Metal electrodes do not adhere to the skin, making them more vulnerable to motion artifacts. In contrast, gel-based wet-contact electrodes (commonly Ag/AgCl) offer a superior ionic conduction interface at the skin-electrode junction [6]. The key difference between these electrode types is their classification as polarizable and non-polarizable. Polarizable electrodes cannot ionize in the salt solution, leading to charge separation due to increased capacitance from potentially oxidized surfaces [7].

Moreover, metal electrodes are influenced by the current characteristics of the skin area and underlying tissue properties. When applied to hands, the outer layer of skin, known as the *stratum corneum* (SC), significantly affects the impedance between skin and electrode. This complex impedance can be represented by capacitance and parallel resistance. The SC resistance R_{sc} typically varies from several $100\,\text{k}\Omega$ to $10\,\text{M}\Omega$ [8]. The capacitance of the SC C_{sc} can be approximated by a cylindrical capacitance described by

$$C_{\text{sc}} = 2\,\pi\,\epsilon_0 \epsilon_r \,\frac{l_{\text{elec}}}{\ln\left(\frac{d_{\text{elec}}+d_{\text{sc}}}{d_{\text{elec}}}\right)}, \tag{1}$$

where ϵ_0 is the vacuum permittivity, l_{elec} and d_{elec} denote the length and the radius of the metal handle electrodes, and d_{sc} is the thickness of the SC of the palm. The SC's relative permittivity ϵ_r ranges from 10^3 to 10^5, depending on humidity conditions, and remains approximately constant across frequencies relevant for ECG analysis [9]. The thickness of the SC d_{sc} varies based on individual characteristics and typically falls between several $10\,\mu\text{m}$ up to $800\,\mu\text{m}$ [10]. For an effective electrode length of $l_{\text{elec}} = 4.5\,\text{cm}$ and a radius of $d_{\text{elec}} = 1.1\,\text{cm}$, capacity calculations suggest a range from $10\,\text{nF}$ to $100\,\mu\text{F}$, influenced by humidity and SC thickness [2].

In addition to these factors, systems that utilize metal electrodes often incorporate actively-driven buffers with high input impedance R_{in} (typically $> 1\,\text{G}\Omega$) and coupling capacities C_{cpl}. In our model, we used $R_{\text{in}} = 25\,\text{G}\Omega$ This configuration creates a passive high-pass filter with cut-off frequencies in the lower Hz range to mitigate baseline wandering. Although this can affect the morphology of the ECG signal, this disadvantage is considered acceptable to enable a more stable measurement. To assess the influences on the ECG signal morphology, the electrical equivalent model shown in Fig. 3 was simulated using MATLAB R2023b Simscape. The recorded reference ECG signal was used as input voltage U_{ecg} into the measurement circuit. The resulting measurement voltage U_{meas} was further analyzed over a large parameter space of C_{cpl} from $0.1\,\text{pF}$ to $100\,\text{pF}$.

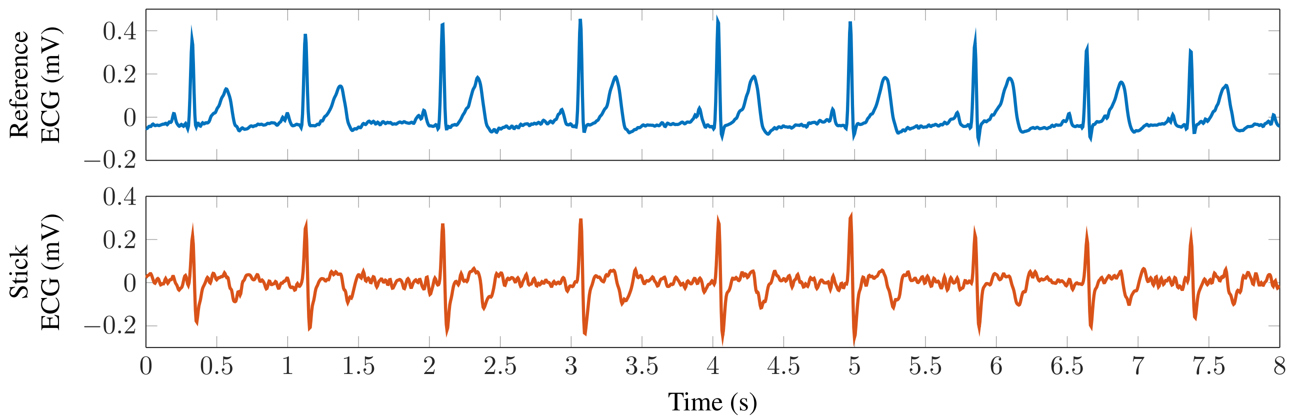

Figure 2. Clinical Einthoven I-lead ECG recording (above) and a synchronized recording of the MyDiagnostick device (below) recorded from a young, healthy subject during deep breathing maneuver.

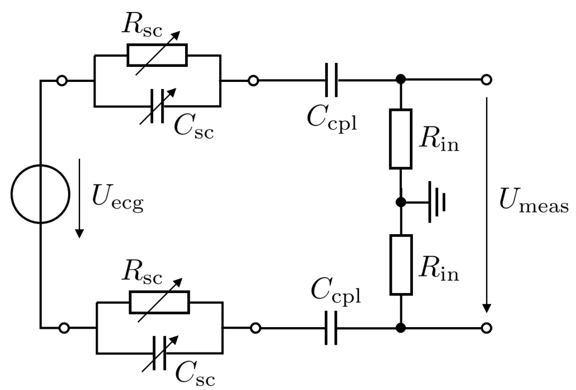

Figure 3. Electrical equivalent circuit of an ECG measurement device incorporating dry electrodes.

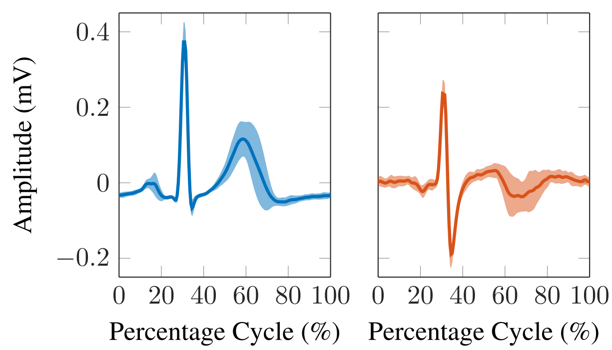

Figure 4. Reference (left) and hand-held device's (right) signal morphologies averaged over heart cycles. Standard deviations are shown in lighter shades.

3. Results

The synchronized recordings of clinical ECG and the hand-held device's ECG reveal significant differences in the signal morphologies when taken from the presumably same Einthoven I-lead (cf. Fig. 2). Therefore, device-related characteristics can be considered accountable for morphological changes. To substantiate this analysis, we have segmented the recordings with respect to the R-peaks and resampled each cycle to calculate the average ECG trajectories for both recordings (cf. Fig. 4). As can be seen, the QRS complex and the T-wave are significantly distorted, as could have been deduced from Fig. 2. However, although not visible for a single heart cycle in Fig. 2, it is also apparent in the average trajectories that the P-wave also appears inverted and delayed.

After forwarding the reference ECG measurements through the simulation model for different configurations of C_{cpl}, we again calculated the average signal morphologies of the resulting output voltages U_{meas}. Afterward, we identified the most likely values for the coupling capacitance by calculating the errors between the simulation output and the average signal trajectory of the device's recording. Therefore, we have used two different metrics: the root mean square error (RMSE), which calculates point-to-point alignment errors without considering temporal shifts, and the dynamic time warping (DTW) distance, which provides the minimum distance between two time-stretched signals. Fig. 5 shows the identified resulting average trajectories for the two different metrics. For RMSE, the identified value for C_{cpl} is $0.9025\,\text{pF}$, whereas for DTW, it is $1.1023\,\text{pF}$, which corresponds to a high-pass cut-off frequency of approx. $6.37\,\text{Hz}$. Therefore, it can be concluded that the implemented electrical equivalent circuit is in close agreement with the real device characteristics.

4. Discussion & Conclusion

In this work, we have analyzed the influence of dry electrodes and the associated signal conditioning stages, typically integrated in handheld devices, on the signal

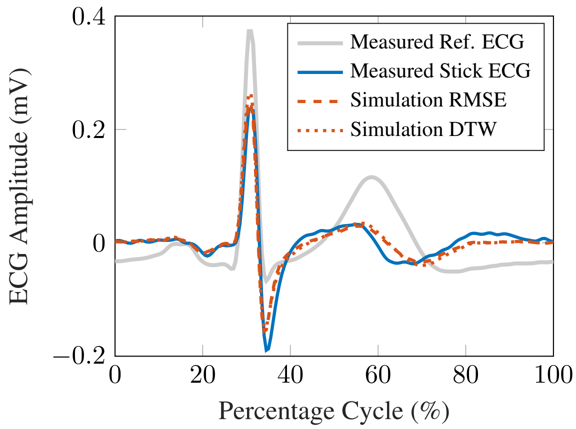

Figure 5. Average signal trajectories from recorded and simulated ECG data. The input signal for the simulation coincides with the reference ECG (gray).

morphology of standard Einthoven I-lead measurements. Qualitative differences can be observed in the signal morphologies from the initial synchronized measurements of both patient monitor and hand-held ECG device, potentially leading to morphological misinterpretation or erroneous calculation of segment intervals. Due to the characteristics of the high-pass filter and the corresponding coupling capacity, the T-wave appears to be inverted at this specific cut-off frequency of the device's input filter stage. This transition results in an earlier isoelectric line. It complicates the reliable measurement of parameters essential for diagnosing other cardiac arrhythmia (PQ interval or ST segment length), limiting additional diagnostic capabilities.

Based on the implemented electrical equivalent circuit model, we conducted further quantitative analyses using the initially recorded ECG data. Simulation results indicate a significant reduction in signal amplitude by approximately one-half of the R-peak amplitude concerning baseline. Previous simulations with an artificial ECG have revealed critical morphological changes with decreasing coupling capacity [2]: an increasingly biphasic P-wave with reduced amplitude, a negative S-peak, and an inverted T-wave. Real measurements suggest that individual skin impedance may render P-waves nearly undetectable in ECG stick measurements (cf. Fig. 2). These findings imply that ECG recordings from large screening devices should be cautiously approached when employing commonly used diagnostic algorithms, including deep neural networks trained on clinical ECG data. Despite these challenges, detecting AF remains achievable by identifying irregular heart rhythms or the absence of clear RR-interval patterns. The MyDiagnostick device's manual supports this approach, noting that classification depends on irregular RR intervals, irrespective of P-wave visibility.

Consequently, further automated analyses will require more sophisticated signal processing techniques to ensure accurate diagnosis. Additionally, comprehensive automated ECG analysis necessitates consistently measured data. The influence of the SC characteristics can be assumed less dominant about the effects of the high-pass characteristic [2]. However, this has not yet been confirmed in more extensive studies, but will be part of our future work on this topic.

References

[1] Zink MD, Mischke KG, Keszei AP, Rummey C, Freedman B, Neumann G, et al. Screen-detected atrial fibrillation predicts mortality in elderly subjects. EP Europace. 2021;23(1):29-38.

[2] Lueken M, Gramlich M, Leonhardt S, Marx N, Zink MD. Automated signal quality assessment of single-lead ecg recordings for early detection of silent atrial fibrillation. Sensors. 2023;23(12):5618.

[3] Pan J, Tompkins WJ. A real-time QRS detection algorithm. IEEE transactions on biomedical engineering. 1985;BME-32(3):230-6.

[4] Desteghe L, Raymaekers Z, Lutin M, Vijgen J, Dilling-Boer D, Koopman P, et al. Performance of handheld electrocardiogram devices to detect atrial fibrillation in a cardiology and geriatric ward setting. Ep Europace. 2017;19(1):29-39.

[5] Diamantino AC, Nascimento BR, Beaton AZ, Nunes MCP, Oliveira KK, Rabelo LC, et al. Atrial fibrillation detection with a portable device during cardiovascular screening in primary care. Heart. 2020;106(16):1261-6.

[6] Chi YM, Jung TP, Cauwenberghs G. Dry-contact and noncontact biopotential electrodes: methodological review. IEEE Reviews in Biomedical Engineering. 2010;3:106-19.

[7] Albulbul A. Evaluating Major Electrode Types for Idle Biological Signal Measurements for Modern Medical Technology. Bioengineering. 2016;3(3):20. Available from: `https://www.mdpi.com/153216`.

[8] Goyal K, Borkholder DA, Day SW. Dependence of Skin-Electrode Contact Impedance on Material and Skin Hydration. Sensors (Basel, Switzerland). 2022;22(21).

[9] Gabriel S, Lau RW, Gabriel C. The dielectric properties of biological tissues: III. Parametric models for the dielectric spectrum of tissues. Physics in medicine and biology. 1996;41(11):2271-93.

[10] Fruhstorfer H, Abel U, Garthe CD, Knttel A. Thickness of the stratum corneum of the volar fingertips. Clinical Anatomy. 2000;13(6):429-33.

Address for correspondence:

Markus Lueken
Medical Information Technology (MedIT)
Helmholtz Institute, RWTH Aachen University
Pauwelsstr. 20, 52074 Aachen, Germany
lueken@hia.rwth-aachen.de